

Adenosine signaling mediates hypoxic responses in the chronic lymphocytic leukemia microenvironment

Sara Serra,^{1,2} Tiziana Vaisitti,^{1,2} Valentina Audrito,^{1,2} Cinzia Bologna,^{1,2} Roberta Buonincontri,^{1,2} Shih-Shih Chen,³ Francesca Arruga,^{1,2} Davide Brusa,² Marta Coscia,⁴ Ozren Jaksic,⁵ Giorgio Inghirami,^{6,7} Davide Rossi,⁸ Richard R. Furman,⁹ Simon C. Robson,¹⁰ Gianluca Gaidano,⁸ Nicholas Chiorazzi,³ and Silvia Deaglio^{1,2}

¹Department of Medical Sciences, University of Turin, Turin, Italy; ²Human Genetics Foundation, Turin, Italy; ³The Feinstein Institute for Medical Research, Northwell Health, Manhasset, NY; ⁴Division of Hematology, Azienda Ospedaliera Città della Salute e della Scienza, Turin, Italy; ⁵Department of Hematology, Dubrava University Hospital, Zagreb, Croatia; ⁶Department of Pathology and Laboratory Medicine, Weill Cornell Medicine, New York, NY; ⁷Department of Molecular Biotechnology and Health Sciences, University of Turin, Turin, Italy; ⁸Division of Hematology, Department of Translational Medicine, University of Eastern Piedmont, Novara, Italy; ⁹Department of Hematology, Weill Cornell Medicine, New York, NY; and ¹⁰Beth Israel Deaconess Medical Center, Harvard University, Boston, MA

Key Points

- Hypoxia shapes the CLL lymph node microenvironment by acting through the A2A adenosine receptor.
- Inhibiting the A2A adenosine receptor counteracts the effects of hypoxia on CLL cells, macrophages, and T lymphocytes.

The chronic lymphocytic leukemia (CLL) niche is a closed environment where leukemic cells derive growth and survival signals through their interaction with macrophages and T lymphocytes. Here, we show that the CLL lymph node niche is characterized by overexpression and activation of HIF-1 α , which increases adenosine generation and signaling, affecting tumor and host cellular responses. Hypoxia in CLL lymphocytes modifies central metabolic pathways, protects against drug-driven apoptosis, and induces interleukin 10 (IL-10) production. In myeloid cells, it forces monocyte differentiation to macrophages expressing IRF4, IDO, CD163, and CD206, hallmarks of the M2 phenotype, which promotes tumor progression. It also induces IL-6 production and enhances nurturing properties. Low oxygen levels decrease T-cell proliferation, promote glycolysis, and cause the appearance of a population of PD-1⁺ and IL-10-secreting T cells. Blockade of the A2A adenosine receptor counteracts these effects on all cell populations, making leukemic cells more susceptible to pharmacological agents while restoring immune competence and T-cell proliferation. Together, these results indicate that adenosine signaling through the A2A receptor mediates part of the effects of hypoxia. They also suggest that therapeutic strategies to inhibit the adenosinergic axis may be useful adjuncts to chemotherapy or tyrosine kinase inhibitors in the treatment of CLL patients.

Introduction

Chronic lymphocytic leukemia (CLL) is characterized by the progressive expansion of a population of monoclonal B lymphocytes expressing CD5 and CD23, which colonize the bone marrow (BM), peripheral blood (PB), and lymph nodes (LNs).¹ A proportion of the leukemic clone renews daily,² with proliferation occurring almost exclusively in LNs.³ It is within anatomic structures (the so-called proliferation centers) found in the LN that CLL cells encounter antigen together with costimulatory signals that drive proliferation and expansion.^{4,5}

Significant advances have been made in the therapy of CLL with the introduction of tyrosine kinase inhibitors. Bruton tyrosine kinase (Btk) and phosphatidylinositol 3-kinase inhibitors achieve long-lasting responses in the majority of patients, improving outcome with relatively limited toxicities.^{6,7} However, these

new drugs do not cure CLL patients. Hence, the identification of drug combinations to treat and ultimately cure the disease is a high priority.

Extracellular nucleotides and nucleosides are part of an evolutionarily conserved and highly sophisticated extracellular network that controls scavenging of precious components, at the same time modulating cellular responses through the activation of different purinergic receptors.⁸ High concentrations of ATP (5-10 mM) are present in the intracellular compartment, whereas low concentrations are typically available extracellularly. However, under conditions of increased cellular turnover and/or inflammation, such as those present in the tumor microenvironment, extracellular nucleotide levels can surge.^{9,10} ATP may then bind specific type 2 purinergic receptors, which activate a signaling cascade, or it may be enzymatically converted to adenosine, a potent immunosuppressant, through a chained reaction controlled by CD39 and CD73 ectoenzymes. CD73, considered rate-limiting in the generation of adenosine,¹¹ is overexpressed by different tumors, including leukemia.^{12,13} Our previous work showed that CD73 is expressed in a subset of CLL cells, which are characterized by clinical and molecular markers of unfavorable prognosis.¹⁴ CD73 expression is dynamically modulated in response to a number of extracellular conditions, including hypoxia, a common feature of the leukemic microenvironment.¹⁵ HIF-1 α and HIF-2 α are the 2 main transcription factors regulated by hypoxia that support tumor progression by activating specific genetic programs.^{16,17} In vivo evidence confirms that hypoxia acts partly through the activation of A2A adenosine receptor signaling.^{18,19} Although circulating CLL cells constitutively express a transcriptionally active HIF-1 α ,²⁰ its role in regulating CLL survival and its mechanisms of action remain incompletely understood.²¹

This work is based on data indicating that adenosine and hypoxia collaborate in modifying the tumor microenvironment in a protolerogenic and tumor-supportive way.^{22,23} Here, we show that CLL cells hosted in proliferation centers of LNs overexpress functional HIF-1 α . In this compartment, genes coding for molecules regulating adenosine production and signaling are upregulated. Our in vitro data indicate that inhibition of the adenosinergic axis restores immune competence, suggesting that it can contribute to CLL eradication in combination with targeted therapies.

Methods

Patient samples and culture conditions

CLL samples were obtained in accordance with institutional guidelines and the Declaration of Helsinki. CLL cells and nurse-like cells (NLCs) were obtained as described in supplemental Methods. Culture conditions were 21% (normoxia) or 1% (hypoxia) O₂, 5% CO₂ at 37°C.

Human CLL xenograft model

The model is described fully in supplemental Methods.

Immunohistochemistry and immunofluorescence microscopy

Formalin-fixed, paraffin-embedded sections of LNs infiltrated by CLL cells and reactive LNs were stained and analyzed as specified in supplemental Methods.

RNA extraction and qRT-PCR

Quantitative real-time PCR (qRT-PCR) was performed using the 7900 HT Fast Real Time PCR System (SDS2.3 software). Gene expression was calculated relative to actin B (RE ACTB). Primers and further details are provided in supplemental Methods.

HPLC measurement of adenosine 5'-monophosphate, adenosine, and inosine

Nucleotide metabolism was analyzed by high-performance liquid chromatography (HPLC), as described in supplemental Methods.

Apoptosis and proliferation assays

Apoptosis was measured using the Annexin V FITC Apoptosis detection kit (Immunostep, Salamanca, Spain). For T-cell proliferation, carboxyfluorescein diacetate succinimidyl ester labeling was performed, as detailed in supplemental Methods.

Flow cytometry, cell sorting, and western blot analysis

Full details are provided in supplemental Methods.

Chemotaxis assay

Chemotaxis experiments were performed on peripheral blood mononuclear cells (PBMCs) from normal donors using Boyden chamber assays, as described previously.²⁴ Full details are in supplemental Methods.

ELISA

Interleukin 6 (IL-6) and IL-10 concentrations in culture supernatants were measured using Quantikine enzyme-linked immunosorbent assay (ELISA) kits (R&D Systems).

Measurement of cell metabolism

Real-time measurements of the extracellular acidification rate (ECAR) were made using an XFp Extracellular Flux Analyzer (Seahorse Bioscience). Full details are in supplemental Methods.

Statistical analyses

Continuous variables were compared using the Mann-Whitney *U* (unpaired data) or Wilcoxon signed rank (paired data) tests. Correlation between continuous variables was assessed using Pearson's correlation coefficients. Full details are in supplemental Methods.

Results

The CLL LN is characterized by HIF-1 α overexpression and activation

Expression levels of HIF-1 α and its direct target, carbonic anhydrase IX (CAIX),²⁵ were comparatively assessed in CLL and reactive LN samples (Table 1). In the CLL LNs, HIF-1 α was intensely positive in areas corresponding to proliferation centers (Figure 1A), where intense reactivity for CAIX was apparent (Figure 1A). Multicolor immunofluorescence confirmed that dividing (Ki-67⁺) CLL (CD23⁺) cells in the proliferation center were CAIX⁺ (supplemental Figure 1A). In contrast, reactive LN obtained from nonleukemic patients showed dim positivity for HIF-1 α and little or no CAIX staining (Figure 1B). In addition, there was an inverse correlation between the intensity of CAIX staining and the distance from the vessels, with cells in perivascular position being significantly less CAIX⁺ than cells in other

Table 1. Characteristics of the CLL LN samples analyzed

Number	Sex	Age, y	Diagnosis	Cytogenetics	LN pattern	PCs
5161	F	67	2004	Del 17p, tri 12	Nodal	Large and confluent
3870	F	78	2013	None	Diffuse	Large
2608	F	55	2014	Del 13q, del 17p	Diffuse	Small
2371	M	67	2010	Del tp53 gene	Nodular	Small
3607	M	50	2013	Tri 12	Cloud/sky	Small
2857	M	86	2013	Del 13q	Diffuse	Large
4557	F	87	2013	None	Diffuse	Small

PCs, proliferation centers.

positions (supplemental Figure 1B). This finding led to the hypothesis that HIF-1 α and CAIX are markers of the level of hypoxia in the CLL LN. Confirmation was obtained using a xenograft model of CLL where human CLL cells and autologous activated T lymphocytes from CLL patients were injected into NOD/SCID/ γ chain^{-/-} (NSG) mice. After 5 weeks, the spleen was infiltrated with large nodules of human CLL cells (CD20⁺) and T lymphocytes (CD3⁺), organized around a central blood vessel. These perivascular aggregates were HIF-1 α ⁺ and CAIX⁺ (Figure 1C; supplemental Figure 1C-D). Multicolor immunofluorescence indicated that both T and B lymphocytes were CAIX⁺ (supplemental Figure 1D). These findings clearly show that leukemic expansion is accompanied by increased expression and activity of the HIF-1 α transcription factor mirroring the human disease. To confirm that HIF-1 α and CAIX are expressed, at least partly, as a consequence of decreased oxygen tension, CLL xenografts were injected with pimonidazole hydrochloride (PIM), a compound that forms covalent bonds with cellular macromolecules at O₂ levels <1.3%.²⁶ Spleen samples recovered for analysis 2 hours after PIM injection showed staining predominantly associated with human perivascular aggregates (Figure 1C, right panel). Consistently, purified human CD45⁺/CD20⁺ CLL cells were also PIM⁺ by flow cytometry and confocal microscopy (Figure 1D).

Lastly, HIF-1 α messenger RNA (mRNA) and protein levels were compared by RT-PCR in the PB, BM, and LNs of paired human CLL patient samples (n = 12). The percentage of leukemic cells in these samples was always >80%. HIF-1 α expression was highest in CLL cells recovered from the LN, as compared with the other 2 compartments (Figure 1E-F), suggesting that genes under the control of HIF-1 α are differentially modulated in the LN vs the BM or PB. Consistently, GLUT1 (*SLC2A1*), lactate dehydrogenase (*LDHA*), and PKM2 (*PKM2*) (supplemental Figure 1E), known HIF-1 α targets,²⁷⁻²⁹ were present at the highest levels in cells obtained from the LN.

Hypoxia promotes adenosine synthesis, scavenging, and signaling in CLL cells

In consideration of the reported bilateral cross-talk between hypoxia-activated HIF-1 α signaling and the adenosinergic axis,^{30,31} we sought to determine whether hypoxia affected expression and function of ATP-degrading enzymes, as well as of adenosine receptors and transporters.

Although freshly purified CLL cells cultured at 1% O₂ did not change HIF-1 α expression at the mRNA level, a marked upregulation of the

protein was evident (supplemental Figure 2A-B). These cells were also stained with anti-CAIX and anti-PIM antibodies (supplemental Figure 2C).

Expression of CD39 and CD73 by CLL cells was compared 48 hours after culture under normoxia or hypoxia in a cohort of 40 CLL patients. CD39 (*ENTPD1*) was highly expressed by leukemic cells^{14,32} and was not significantly modulated by hypoxia (Figure 2A, left panel). On the contrary, CD73 (*NT5E*) expression varied considerably among patients, as expected.¹⁴ In the subset with >30% CD19⁺/CD73⁺ CLL cells (n = 17), hypoxia invariably increased CD73 mRNA expression (Figure 2A, right panel), while the modifications in the negative subset were not significant (supplemental Figure 3A). In the >30% subset, we observed a positive correlation between *NT5E* and *HIF1A* mRNA levels (supplemental Figure 3B), in line with data indicating a direct transcriptional control of *NT5E* by HIF-1 α .¹⁵ No association was apparent in the CD73⁻ subset (supplemental Figure 3C), suggesting that other regulatory mechanisms are in place.

At the protein level, CD39 was not significantly different in normoxic or hypoxic conditions (Figure 2B, left panel), whereas the mean fluorescence intensity of CD73 increased under hypoxia, specifically in the positive subset (Figure 2B, right panel). In consideration of the variability in CD73 expression and responses to HIF-1 α activation, attention was focused specifically on the positive samples. Here, the adenosine 5'-monophosphate (AMP)-degrading activity controlled by CD73 was upregulated in hypoxic CLL cells (Figure 2C; supplemental Figure 4A). However, no significant increase in adenosine production was detected under hypoxic conditions (Figure 2C-D). Since this finding could indicate that adenosine is further degraded to inosine, a reaction controlled by the enzyme adenosine deaminase, this hypothesis was tested and documented. We found that hypoxia promoted transcription and expression of CD26 (*DPP4*; Figure 2E), which is a molecular anchor for adenosine deaminase.³³ This expression profile suggested that under hypoxic conditions, CLL cells upregulate the enzymatic machinery for ATP scavenging, with degradation of ATP to inosine and subsequent cellular uptake. Consistently, HPLC measurements of substrates and products confirmed inosine accumulation under hypoxia (Figure 2C-F). A net increase in adenosine production occurred only after inhibiting adenosine deaminase using *erythro*-9-(2-hydroxy-3-nonyl)adenine (EHNA; Figure 2C-D). Furthermore, RT-PCR studies showed significant upregulation of the genes coding for equilibrative nucleoside transporters ENT1 and ENT2 (*SLC29A1* and *SLC29A2* genes; Figure 2G), indicating that adenosine and inosine can be internalized. Expression of the A2A adenosine receptor (*ADORA2A*) was also markedly increased in hypoxic CLL cells (Figure 2H), while the other adenosine receptors remained expressed at very low levels (not shown). In line with the presence of a functional A2A receptor, crosslinking with the specific A2A agonist CGS21680 increased intracellular cyclic AMP (cAMP) levels, which were maximal in cells cultured under hypoxia (supplemental Figure 5).

We then compared gene expression profiles of CLL cells obtained concurrently from a single patient's PB or LNs. The BM could not be included in this analysis because of limited sample availability. The results showed induction of *NT5E*, *DPP4*, *SLC29A1*, and *ADORA2A* in the LN samples (Figure 2I). Under these conditions, *ENTPD1* was also upregulated, suggesting that the adenosine-producing capability is further enhanced in vivo. Upregulation of A2A suggests that adenosine signaling is active in the LN.

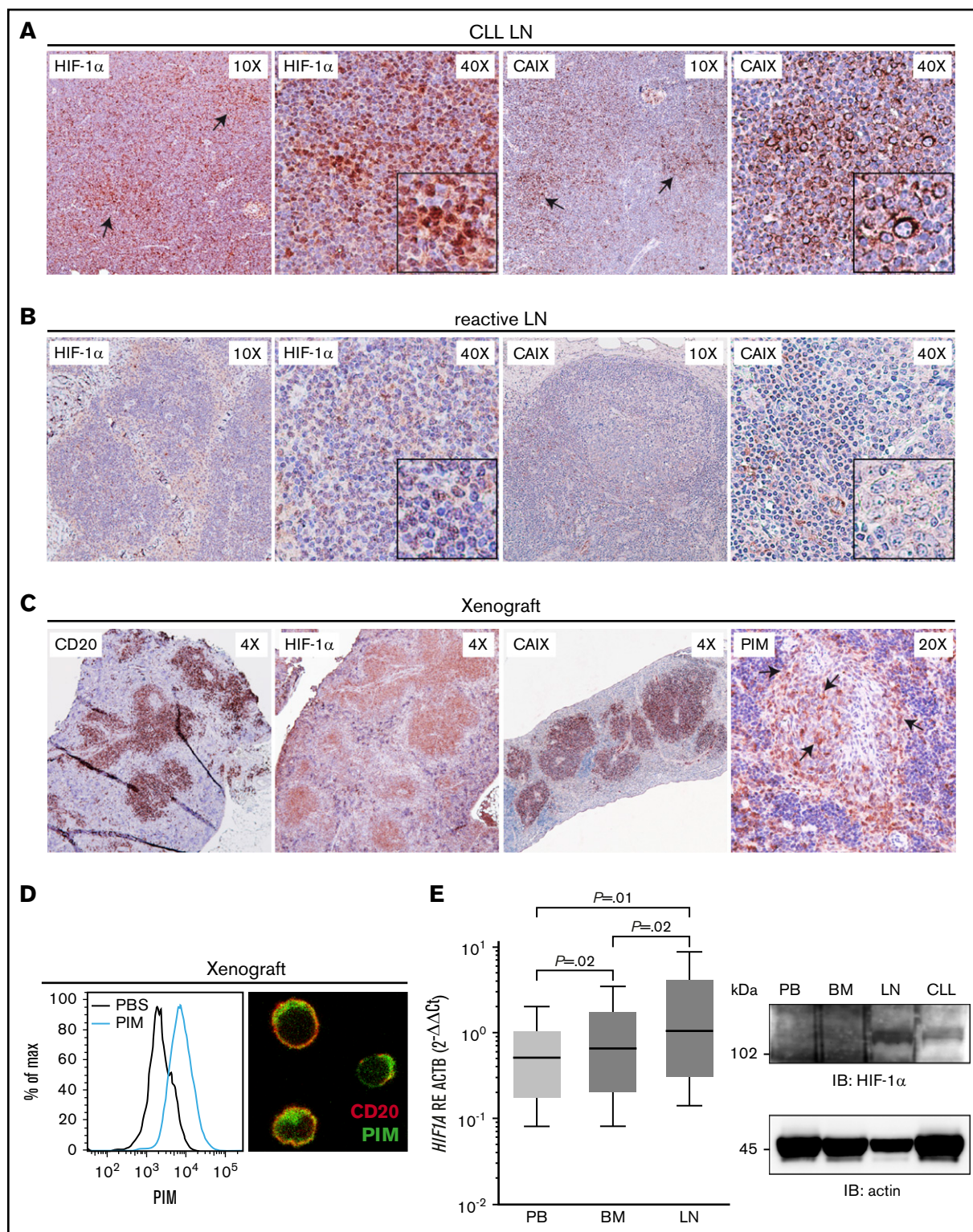


Figure 1. The CLL proliferation center is a hypoxic environment. (A) Immunohistochemistry of a representative ($n = 7$) CLL LN sample stained with anti-HIF-1 α and anti-CAIX antibodies, with more intense signal localized in proliferation centers (black arrows). Original magnification $\times 10$ and $\times 40$. (B) The same antibodies were used to stain reactive LN samples ($n = 3$), showing dim positivity in correspondence of lymphocytes. Original magnification $\times 10$ and $\times 40$. (C) Spleen samples ($n = 6$) obtained from CLL xenografts in NSG mice stained with anti-human CD20 to show CLL cells (left panel). The middle panels show HIF-1 α and CAIX staining of xenografted mice spleen sections with strong positivity in the areas colonized by human cells. NSG mice xenografted with human CLL cells were injected with 100 mg/kg pimonidazole (PIM). Spleen specimens, obtained 2 hours after injection, were fixed and stained with an anti-PIM antibody (right panel). Original magnification $\times 4$ and $\times 20$. (D) Human cells recovered from the spleen of mice bearing CLL xenografts and injected with PIM were stained with anti-human CD45, CD20 and anti-PIM antibodies before flow cytometry and confocal microscopy analysis (original

Together, these results indicate that CLL cells adapt to hypoxia by upregulating HIF-1 α signaling, in turn increasing nucleotide scavenging and activating adenosine signaling through the A2A receptor.

Hypoxia, acting through the A2A receptor, induces metabolic adaptation of CLL cells, triggering protection from drug-induced apoptosis and production of IL-10

When deprived of oxygen, tumor cells quickly promote energy production through glycolysis.^{34,35} This metabolic adaptation is transcriptionally mediated by HIF-1 α . In addition, several reports indicate that signaling through the adenosine receptors can stabilize HIF-1 α , activating metabolic responses.^{36,37} Here, we observed that culture of CLL cells under hypoxic conditions was followed by significant modifications in basic metabolic processes. In agreement with published data,^{38,39} we observed that under normoxia, CLL cells predominantly obtain energy through oxidative phosphorylation (data not shown). However, at 1% O₂, CLL cells markedly increased expression of genes involved in glycolysis, including the glucose transporter GLUT1, the lactate transporter monocarboxylate transporter 4 MCT4 (*SLC16A3*), *LDHA*, and *PKM2*, all of which control key steps in glycolysis (Figure 3A). Dynamic monitoring of metabolic responses confirmed a sharp increase in glycolysis, as observed in purified cells from 8 patients (Figure 3B). The glycolytic capacity and total glycolytic flux, which are extremely low under normoxic conditions, rose sharply when CLL cells were cultured in 1% O₂ for 48 hours. Addition of the A2A inhibitor to hypoxic cell cultures almost completely inhibited this metabolic adaptation, directly linking adenosine signaling to central metabolic programs (Figure 3B; supplemental Figure 4B). Hypoxia-induced metabolic changes impinge on vital cellular functions, as previously shown for macrophages and T lymphocytes,^{40,41} where a shift to glycolysis increased survival. Furthermore, A2A signaling in CLL was related to protection from apoptosis.¹⁴ These 2 observations prompted us to ask whether hypoxia protected from drug-induced apoptosis and, if so, whether this effect was A2A mediated. Data indicate that apoptosis induced by ibrutinib, a Btk inhibitor with considerable efficacy in this disease, or by fludarabine, one of the most commonly used chemotherapeutics, was significantly reduced under hypoxia (Figure 3C; supplemental Figure 6A). No modification in the expression of Btk under hypoxia was apparent (supplemental Figure 6B). The A2A-specific antagonist SCH58261 restored toxicity of ibrutinib or fludarabine on CLL cells, confirming that the effect is mediated at least partly through the A2A receptor (Figure 3C).

Lastly, within tumors, both hypoxia and adenosine have immunosuppressive functions mediated through cytokine secretion, including

IL-10,^{35,42} and a glycolytic switch was recently associated to the acquisition of a regulatory phenotype in T cells.^{41,43} In keeping with these observations, CLL cells cultured under hypoxia sharply upregulated *IL10* mRNA (Figure 3D), the hallmark cytokine of regulatory B cells.⁴⁴ This upregulation appeared partly mediated through A2A signaling, as receptor blockade with SCH58261 prevented IL-10 increase. Consistently, a high number of IL-10⁺ CLL cells were detected in CLL LN, in contrast to reactive LN sections (Figure 3E-G). The IL-10⁺ population was clearly labeled by B-cell (CD20, full arrows) and T-cell (CD2, open arrow) markers and included proliferating (Ki-67⁺) cells (Figure 3G, arrowheads).

In conclusion, lowering oxygen tension in CLL cells is followed by a metabolic shift to glycolysis, which favors survival and the acquisition of a B-regulatory phenotype, mediated, at least in part, through A2A.

Hypoxia induces adenosine production in macrophages

Macrophages are key components of the microenvironmental architecture of CLL.⁴⁵ They are also termed NLCs, exhibit the hallmarks of alternatively activated or type 2 macrophages (M2), and secrete cytokines supporting tumor growth and suppressing immune responses.^{46,47}

Comparative analysis of the expression of ATP-metabolizing enzymes in NLC revealed dramatic upregulation of CD73 under hypoxia (Figure 4A). CD39 and CD26 were constitutively expressed at high levels and were not significantly modulated by hypoxia (Figure 4B). Consistently, supernatants from NLC cultures challenged for 30 minutes with extracellular AMP showed marked upregulation of adenosine concentrations, in contrast to their normoxic counterparts (Figure 4C). Addition of the adenosine deaminase inhibitor EHNA further increased adenosine production, suggesting that part of the product is then converted to inosine (Figure 4C).

Both mRNA and protein levels of A2A were markedly increased under hypoxia (Figure 4D), while in CLL LNs, levels showed a distribution similar to those of CD68 (supplemental Figure 7A). Multicolor confocal immunofluorescence indicated that A2A and CD68 were coexpressed (Figure 4E). A subset of CD23⁺ B cells also stained positive for the A2A receptor, confirming the gene profiling data (Figure 4E). Furthermore, treatment of NLCs with the A2A agonist was followed by activation of AKT/phosphatidylinositol 3-kinase and MAP kinases (Figure 4F), suggesting that the receptor is functional. Phosphorylation of STAT3 and nuclear localization of p65 subunit of the NF- κ B complex was detected, consistent with activation of transcription (Figure 4F-G).

Figure 1. (continued) magnification $\times 63$. (E) RT-PCR analysis of HIF-1 α (*HIF1A*) expression in PB, BM, or LN CLL cells obtained concurrently from the same patient shows higher expression in LN than in the PB or BM ($n = 12$). The Wilcoxon signed rank test was used for comparative analyses. Panel on the right shows western blot analysis for HIF-1 α expression in lysates obtained from the PB, BM, and LN of paired samples. Lysates were obtained by pooling cells obtained from 5 samples. The last lane on the right shows a positive control obtained after culturing purified CLL cells for 48 hours under hypoxia. Immunohistochemical samples were analyzed using an AXIO Laboratory.A1 microscope (Zeiss, Milan, Italy) equipped with a Canon EOS600D and images acquired with the ZoomBrowserEx software (Canon). Immunofluorescence was analyzed using a TCS SP5 laser scanning confocal microscope with an oil immersion 63 \times 1.4 objective lens (Leica Microsystems, Milan, Italy). Images were acquired using the LAS AF version Lite 2.4 software (Leica Microsystems) and processed with Adobe Photoshop (Adobe Systems). IB, immunoblot.

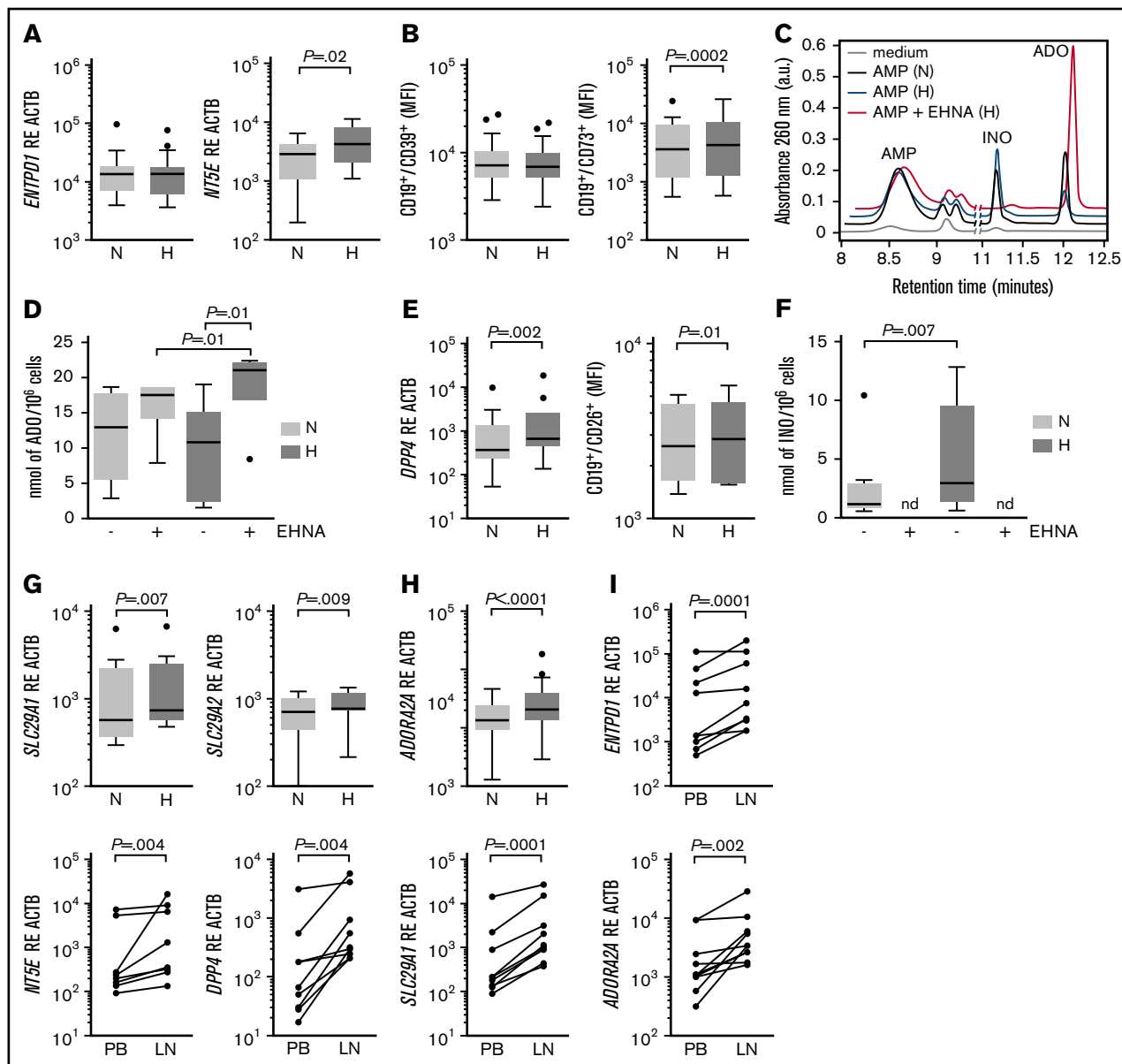


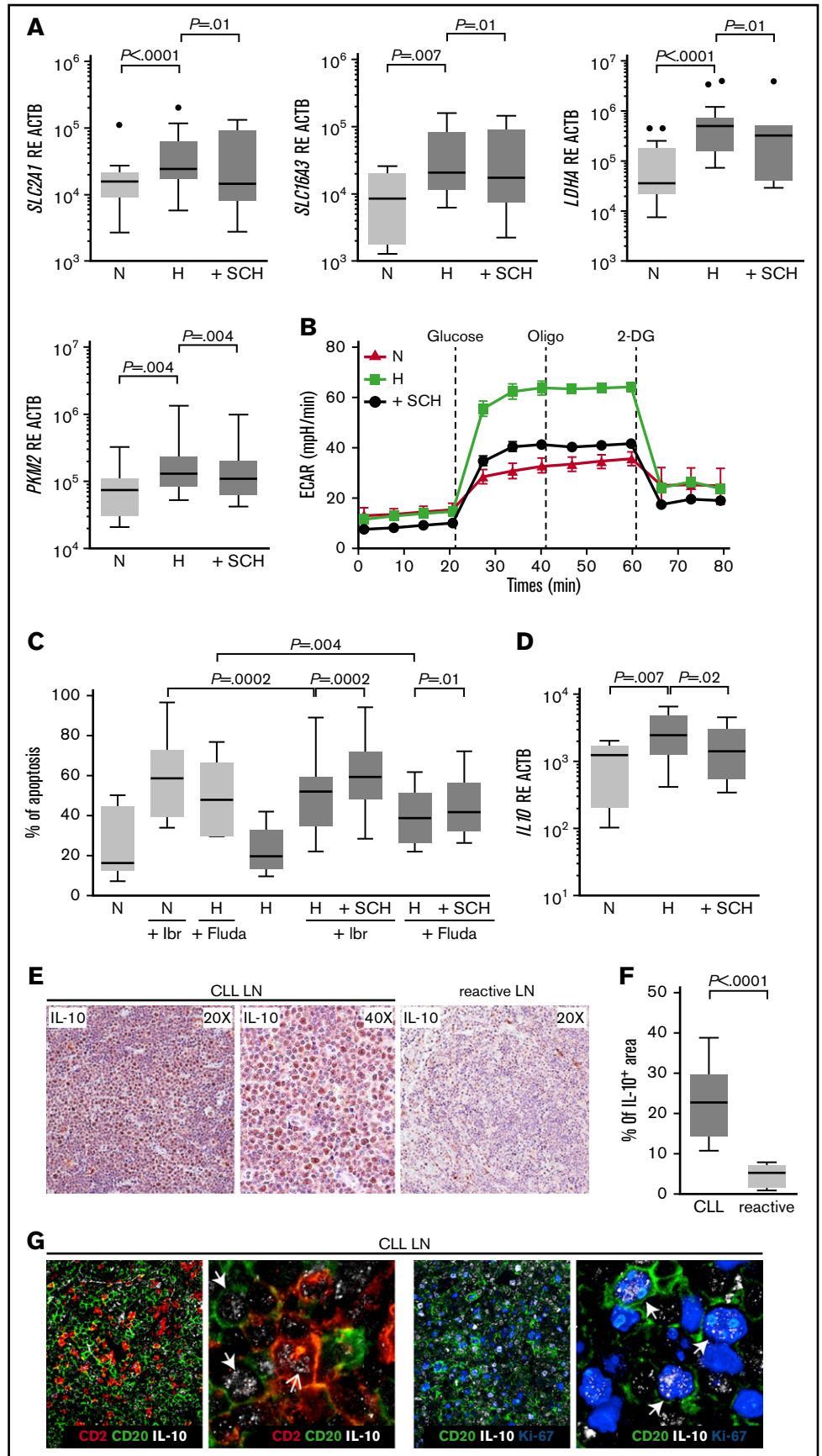
Figure 2. Hypoxia upregulates the adenosinergic axis in CLL cells. (A) RT-PCR data or (B) mean fluorescence intensity (MFI) and protein levels of CD39 (*ENTPD1*) or CD73 (*NT5E*) expression in CLL cells cultured for 48 hours under normoxic or hypoxic conditions. For CD73 analysis, only the patients that were $>30\%$ CD73 $^{+}$ at the baseline (17/40) were analyzed. (C) HPLC chromatogram showing adenosine monophosphate (AMP) catabolism in CLL lymphocytes under normoxia (black line) or hypoxia (blue line) and in the presence of the adenosine deaminase inhibitor EHNA (red line). The gray line profile represents the medium alone. (D) Boxplots showing nanomoles of adenosine produced by 10^6 purified CLL cells after 30 minutes of normoxic or hypoxic culture in the presence of 200 μM AMP ($n = 8$). The adenosine deaminase inhibitor EHNA (10 μM , 30 min, 37°C) was added where indicated ($n = 8$). (E) Comparative expression of CD26 (*DPP4*) mRNA ($n = 10$) and surface protein levels ($n = 10$) in circulating CLL lymphocytes under normoxia or hypoxia. (F) Boxplots representing nanomoles of inosine (INO) accumulated by 10^6 purified CLL cells cultured for 30 minutes in the presence of 200 μM AMP under normoxia or hypoxia. The adenosine deaminase inhibitor EHNA was added where indicated ($n = 8$). (G-H) RT-PCR data of ENT1 (*SLC29A1*, $n = 10$) and ENT2 (*SLC29A2*, $n = 10$) nucleoside transporters and A2A receptor (*ADORA2A*, $n = 20$) expression under normoxic or hypoxic conditions. (I) RT-PCR data comparing expression of CD39 (*ENTPD1*), CD73 (*NT5E*), CD26 (*DPP4*), ENT1 (*SLC29A1*), and A2A receptor (*ADORA2A*) mRNA in the PB or LN of samples obtained concurrently from 9 different patients. Expression was significantly higher in CLL cells obtained from the LN than in paired PB samples. Statistical analyses were performed with the Wilcoxon signed rank test followed by Tukey test. a.u., arbitrary units; ADO, adenosine; INO, inosine; H, hypoxia (dark gray boxes); N, normoxia (light gray boxes).

A2A activation recapitulates the effects of hypoxia in the differentiation of M2 macrophages

Culture under hypoxia of PBMCs from CLL patients markedly increased the numbers of adherent myeloid cells, as determined by Giemsa and CD68 staining (Figure 5A; supplemental Figure 6B).

Continuous A2A activation, obtained by adding CGS21680 every 48 hours, mimicked the effects obtained under hypoxia. Conversely, NLC differentiation was inhibited by addition of SCH58261 antagonist to hypoxic PBMC cultures (Figure 5A; and supplemental Figure 6B). Furthermore, A2A ligation enhanced expression of M2 markers, including

Figure 3. Hypoxia induces metabolic adaptation in CLL cells, triggering protection from drug-induced apoptosis and production of IL-10 in an A2A-dependent manner. (A) RT-PCR analyses of GLUT1 (*SLC2A1*), MCT4 (*SLC16A3*), LDH (*LDHA*), and PKM2 (*PKM2*) in CLL cells under normoxia or hypoxia (n = 17). Where indicated, cells were treated with the A2A antagonist SCH58261 (10 μM). (B) Representative glycolytic profile obtained by dynamic measurement with the Seahorse in CLL cells cultured under normoxic (red triangles and line) or hypoxic (green squares and line) conditions or hypoxic conditions in the presence of the A2A antagonist SCH58261 (black dots and line). (C) Boxplot showing the percentage of apoptotic cells under normoxia or hypoxia. The A2A antagonist was added to block A2A signaling under hypoxia. Where indicated, cells were treated with ibrutinib (10 μM) or fludarabine (5 μM) before assessing apoptosis (n = 16). (D) RT-PCR data showing the IL-10 mRNA expression on CLL cells cultured under normoxic or hypoxic conditions in the presence of CpG/IL-2. Where indicated, leukemic cells were treated with SCH58261 (10 μM). (E-G) Immunohistochemical (E) and immunofluorescence (G) analyses of IL-10 expression in CLL and reactive LNs. Boxplot showing the percentage of IL-10⁺ area quantified in 10 independent fields from 4 CLL LNs or 3 reactive LNs (F). CD2 (red, open arrow) was used as a T-cell marker; CD20 (green) and Ki-67 (blue, full arrows) stained positive CLL lymphocytes (G). Original magnification ×20, ×40, and ×63. Statistical analyses were performed with the Wilcoxon signed rank and Mann-Whitney U tests. Quantification of brown signal in immunohistochemical analysis was performed with the LAS version 3.8 software (Leica Microsystems). Fluda, fludarabine; H, hypoxia (dark gray boxes); Oligo, oligomycin; Ibr, ibrutinib; N, normoxia (light gray boxes); SCH, SCH58261; 2-DG, 2-deoxy-D-glucose.



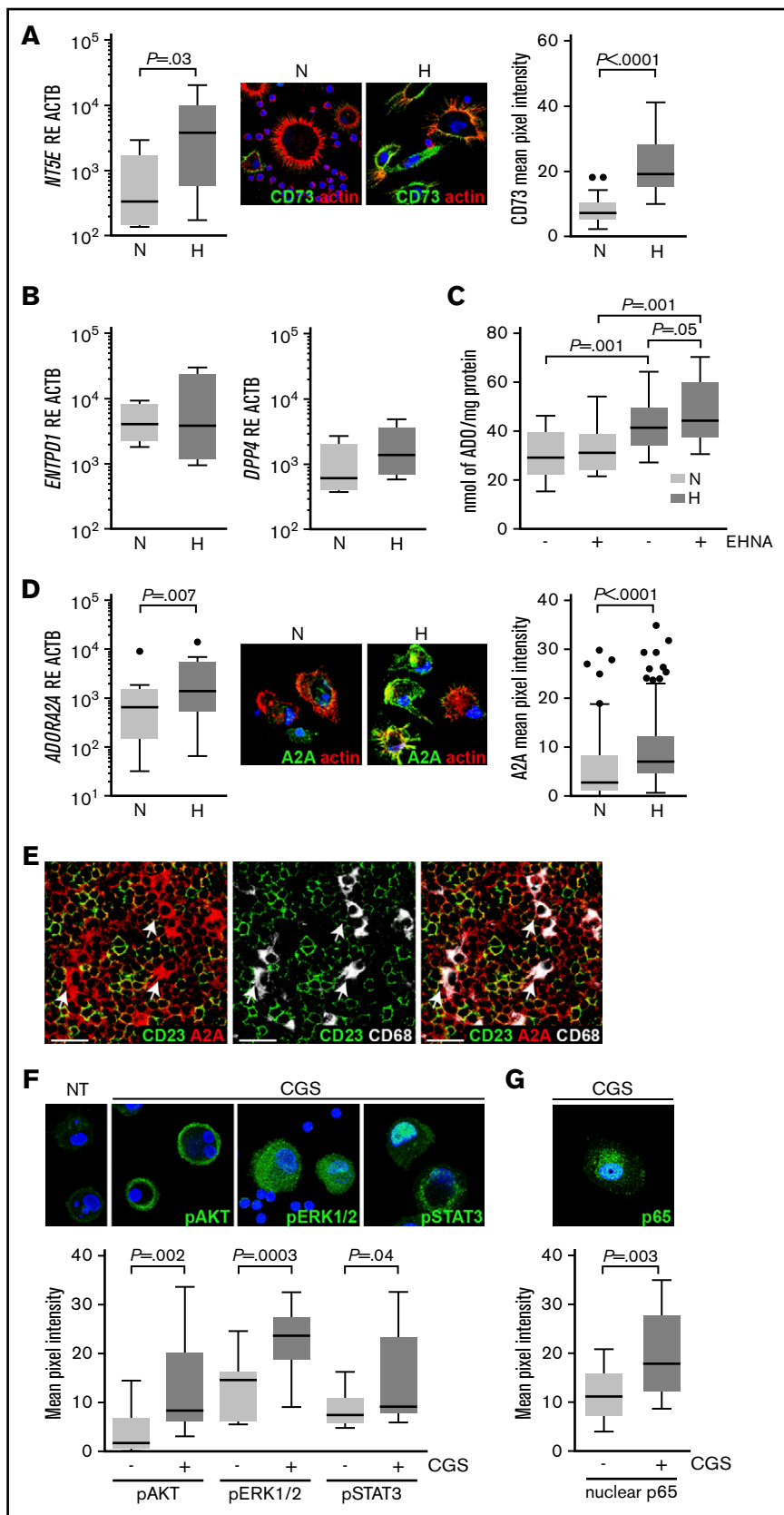


Figure 4. Hypoxia induces adenosine production and signaling in NLCs derived from CLL patients. (A) RT-PCR analysis of CD73 (*NT5E*, $n = 9$, left panel) and immunofluorescence confocal microscopy (right panels) of CD73 surface expression on NLCs generated from CLL patients under normoxic or hypoxic conditions. Cumulative data of CD73 mean pixel intensity confirmed a robust increase in expression under hypoxia. Original magnification $\times 63$. (B) RT-PCR data on CD39 (*ENTPD1*) and CD26 (*DPP4*) expression indicated that NLCs are constitutively CD39⁺ and CD26⁺ but fail to significantly modulate the 2 molecules under hypoxia ($n = 9$). (C) HPLC analysis showing increased adenosine accumulation in NLCs exposed to 200 μM AMP (30 min, 37°C) under hypoxia ($n = 11$). Pretreatment with the adenosine deaminase inhibitor EHNA (10 μM , 30 min, 37°C) further increased adenosine production. (D) RT-PCR analysis of A2A (*ADORA2A*, left panel, $n = 9$) and immunofluorescence confocal microscopy (right panels) of the A2A receptor on NLC under normoxia or hypoxia. Cumulative data of A2A mean pixel intensity from 7 different experiments obtained by quantifying green fluorescence intensity in 3 randomly chosen fields using the ImageJ software. Original magnification $\times 63$. (E) Immunohistochemical (left panel) and confocal microscopy analyses (right panels) of A2A and CD68 expression in LN sections showed enhanced staining in CLL proliferation centers, particularly by CD68⁺ myeloid cells. Triple staining with anti-CD23 (green), anti-A2A (red), and anti-CD68 (white) shows that CD68⁺ cells are strongly A2A⁺ (white arrows). Original magnification $\times 63$. Scale bars, 25 μm . (F-G) Ligation of the A2A receptor with the pharmacological agonist CGS21680 (10 μM , 30 min, 37°C) in NLCs under normoxic conditions is followed by the phosphorylation of AKT, ERK1/2, STAT3 (F, top panels) and p65 (G, top panel). Original magnification $\times 63$. The boxplots (F-G, bottom panels) show cumulative data of mean pixel intensity from NLC preparations obtained from 5 different patients. p65 activation was measured considering immunofluorescence within the nuclei, identified by DAPI staining. Statistical differences were analyzed using the Wilcoxon signed rank test and the Mann-Whitney *U* tests followed by the Tukey test. ADO, adenosine; CGS, CGS21680; H, hypoxia (dark gray boxes); N, normoxia (light gray boxes); SCH, SCH58261.

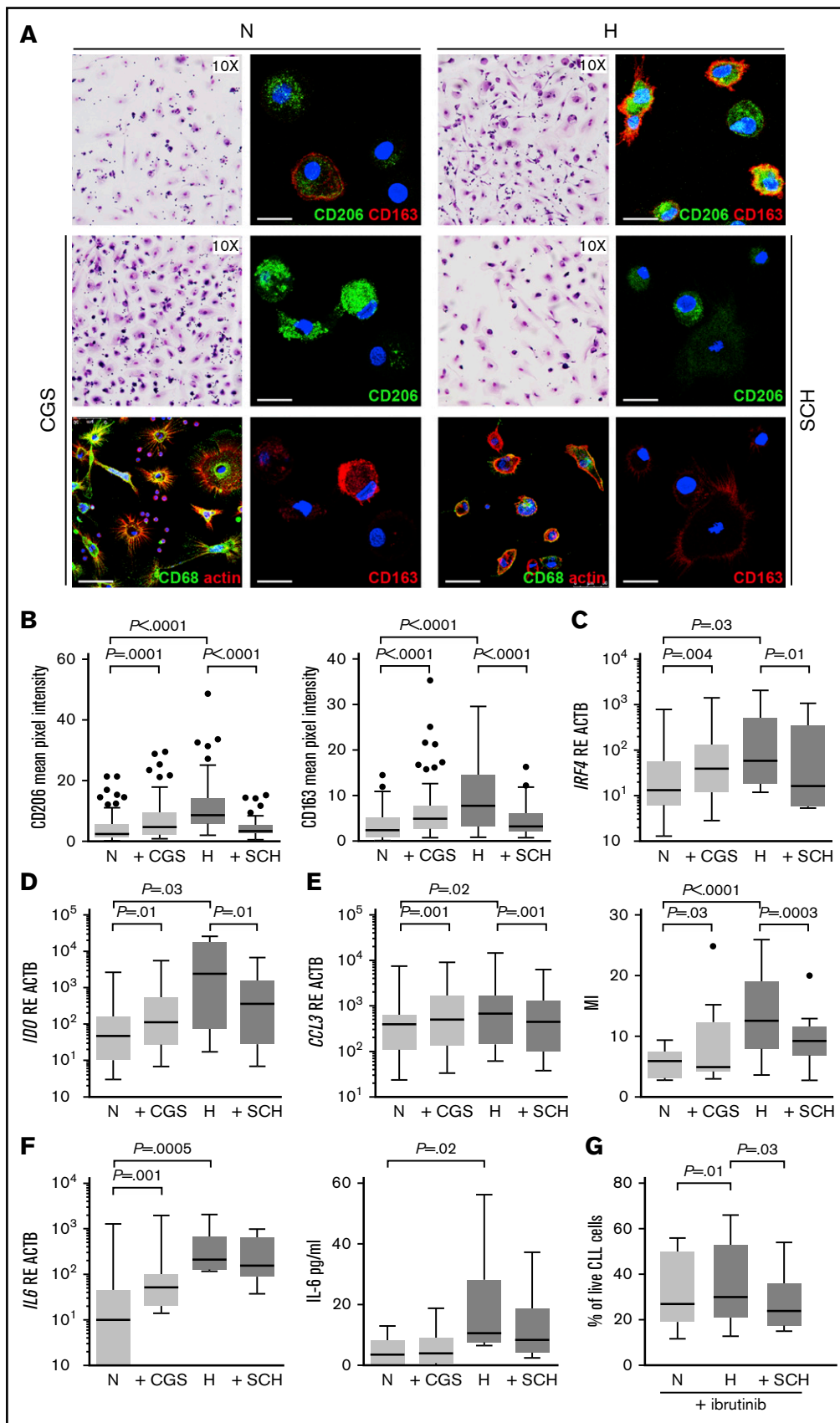


Figure 5.

CD206 and CD163, paralleling the effects exerted by hypoxia (Figure 5A-B). Inhibition of expression of these markers by the A2A antagonist showed that the effects of hypoxia were partly mediated through the activation of the adenosinergic axis (Figure 5A-B).

Gene expression profiling revealed upregulation in hypoxic conditions of the interferon regulatory factor 4 (*IRF4*) transcription factor (Figure 5C), a master regulator of M2 differentiation, and of the tryptophan-metabolizing enzyme indoleamine 2,3-dioxygenase (*IDO*), an immunomodulatory enzyme produced by M2 macrophages (Figure 5D).⁴⁸ Culture with the antagonist prevented their overexpression, confirming that these effects are mediated through A2A (Figure 5C-D). We also detected a marked upregulation in *CCL3* mRNA (Figure 5E), suggesting that the increased number of differentiated macrophages upon hypoxia depends on increased recruitment of myeloid cells. In line with this hypothesis, chemotaxis of normal monocytes was maximal toward spent media of NLCs cultured under hypoxia. Furthermore, chemotaxis was increased in the presence of the A2A agonist and prevented by the antagonist (Figure 5E). Likewise, synthesis of IL-6, which provides growth signals to CLL cells, was increased under hypoxia (Figure 5F). All these effects were mimicked by the A2A agonist under normoxia and prevented using the antagonist (Figure 5E-F).

Lastly, NLCs differentiated under hypoxia were stronger supporters of CLL cell survival than those differentiated under normoxia. This was evident in normal conditions (data not shown) and upon treatment with ibrutinib (Figure 5G). Exposure to the A2A antagonist decreased leukemia cell survival, albeit incompletely, further supporting the hypothesis that the adenosinergic axis mediates the hypoxic phenotype.

Hypoxia suppresses T-cell responses and induces regulatory T cells in an A2A-dependent manner

To address the role of hypoxia in the T-cell compartment, PBMCs from CLL patients were cultured under 21% or 1% O₂ in the presence of anti-CD3/CD28 activating antibodies and IL-2. After T-cell expansion for 5 to 7 days, CD19⁻/CD5⁺ lymphocytes were sorted and used for further studies. Analysis of CD3 expression confirmed that >95% of these cells were T lymphocytes (supplemental Figure 8A).

CD4⁺ and CD8⁺ T lymphocytes activated with anti-CD3/CD28 activating antibodies proliferated significantly less under hypoxia than under normoxia (Figure 6A; supplemental Figure 8B). The dramatic increase in A2A expression under low O₂ tension (supplemental Figure 8C) suggested that inhibition of T-cell proliferation was obtained through the adenosinergic axis, as shown previously.⁴⁹ Consistently, ligation of the A2A under hypoxia further decreased T-cell proliferation, while the SCH58261 antagonist partially rescued it (Figure 6A; supplemental Figure 8B).

Hypoxia markedly modified central metabolic pathways, with upregulation of the glucose and lactate transporters and of *LDHA* and *PKM2* (Figure 6B). This phenotype indicates a metabolic switch toward reliance on glycolytic mechanisms, which are linked to antigen-specific T-cell activation.^{50,51} Similarly, after dynamic measurement of the ECAR, we found that hypoxic T cells increased their basal and maximal glycolysis more than normoxic ones (Figure 6C). The A2A antagonist prevented these changes, indicating that the receptor participates in the metabolic adaptation of T lymphocytes (Figure 6B-C).

Activation of glycolysis promotes the development of a population of T cells with a regulatory phenotype and suppressive properties.^{41,43} Accordingly, the percentage of T cells with a CD4⁺/CD25^{high}/CD127^{low} was higher in hypoxic than normoxic cultures of PBMC, without any activation (Figure 7A). Likewise, activation of CLL T lymphocytes under hypoxia increased expression of the FoxP3 transcription factor (*FOXP3*; Figure 7B). The finding of significantly higher numbers of FoxP3⁺ regulatory T cells (Tregs) in the CLL LN than in reactive specimens (Figure 7C) pointed to a role of HIF-1 α signaling in directing T-cell differentiation in the CLL LN. Expansion of Tregs under these conditions could be due, at least in part, to the documented upregulation of transforming growth factor β (TGF- β), which causes the conversion of naive T cells into Tregs⁵² (Figure 7D). In keeping with a suppressive phenotype of hypoxic T cells, interferon γ (*IFNG*) mRNA levels were significantly reduced (Figure 7E). Lastly, hypoxia robustly induced PD-1 (*PDCD1*), IL-10 (*IL10*), and vascular endothelial growth factor (*VEGFA*) expression and secretion by activated T cells (Figure 7F-G; supplemental Figure 9A), suggesting that their suppressive effects are exerted through cell-bound and soluble mechanisms. Confocal microscopy confirmed that within the CLL LN a high proportion of CD4⁺ T cells express the immunoinhibitory receptor PD-1 (Figure 7F; supplemental Figure 9B).⁵³ Moreover, the finding of a population of

Figure 5. Hypoxia forces M2 differentiation of CLL monocytes through the A2A adenosine receptor. (A) Representative Giemsa staining (left panels) obtained after 12- to 14-day cultures of PBMCs from 8 CLL patients. Where indicated, cultures were performed in the presence of the A2A agonist CGS21680 or antagonist SCH58261 (both 1 μ M, added every 48 hours). Macrophage differentiation was confirmed by staining with the lineage-specific marker CD68 (green). Slides were counterstained with Alexa Fluor 568-conjugated phalloidin (red) and DAPI (blue). Expression of the M2 macrophage markers CD206 (green) and CD163 (red) was evaluated in the same samples. Original magnification $\times 10$ (Giemsa staining) and $\times 63$ (confocal microscopy). Scale bars represent 50 and 25 μ m for the CD68 and CD206/CD163 panels, respectively. (B) Boxplots show cumulative mean pixel intensity data in CD206 (left) and CD163 (right) obtained from at least 5 measurements in 3 different random fields for each of the 6 samples analyzed. (C-F) RT-PCR data showing expression of the interferon regulatory factor 4 (*IRF4*; C) transcription factor, the enzyme indoleamine 2,3-dioxygenase (*IDO*; D), the *CCL3* chemokine (*CCL3*; E), and IL-6 (*IL6*; F) in NLC preparations obtained in 21% or 1% O₂, in the presence of A2A agonists and antagonists (both at 1 μ M, added every 48 hours throughout the 12- to 14-day differentiation process, n = 10). (E) Boxplot on the right represents cumulative data of the migration index (MI) calculated on CD14⁺ cells from normal donors in the presence of NLC spent media. (F) Increased expression of IL-6 was confirmed by checking protein concentrations in culture supernatants using an ELISA assay (right panel). (G) Boxplot showing the percentage of live CLL cells in coculture with NLCs obtained under normoxic or hypoxic conditions. After the differentiation period, autologous purified CLL cells were thawed and plated over the NLC layer and cultured for 48 hours under normoxia or hypoxia. Apoptosis was evaluated by staining with Annexin V and propidium iodide (n = 7). The Wilcoxon signed rank and Mann-Whitney U tests, followed by the Tukey test, were used for statistical analyses. CGS, CGS21680; H, hypoxia (dark gray boxes); N, normoxia (light gray boxes); SCH, SCH58261.

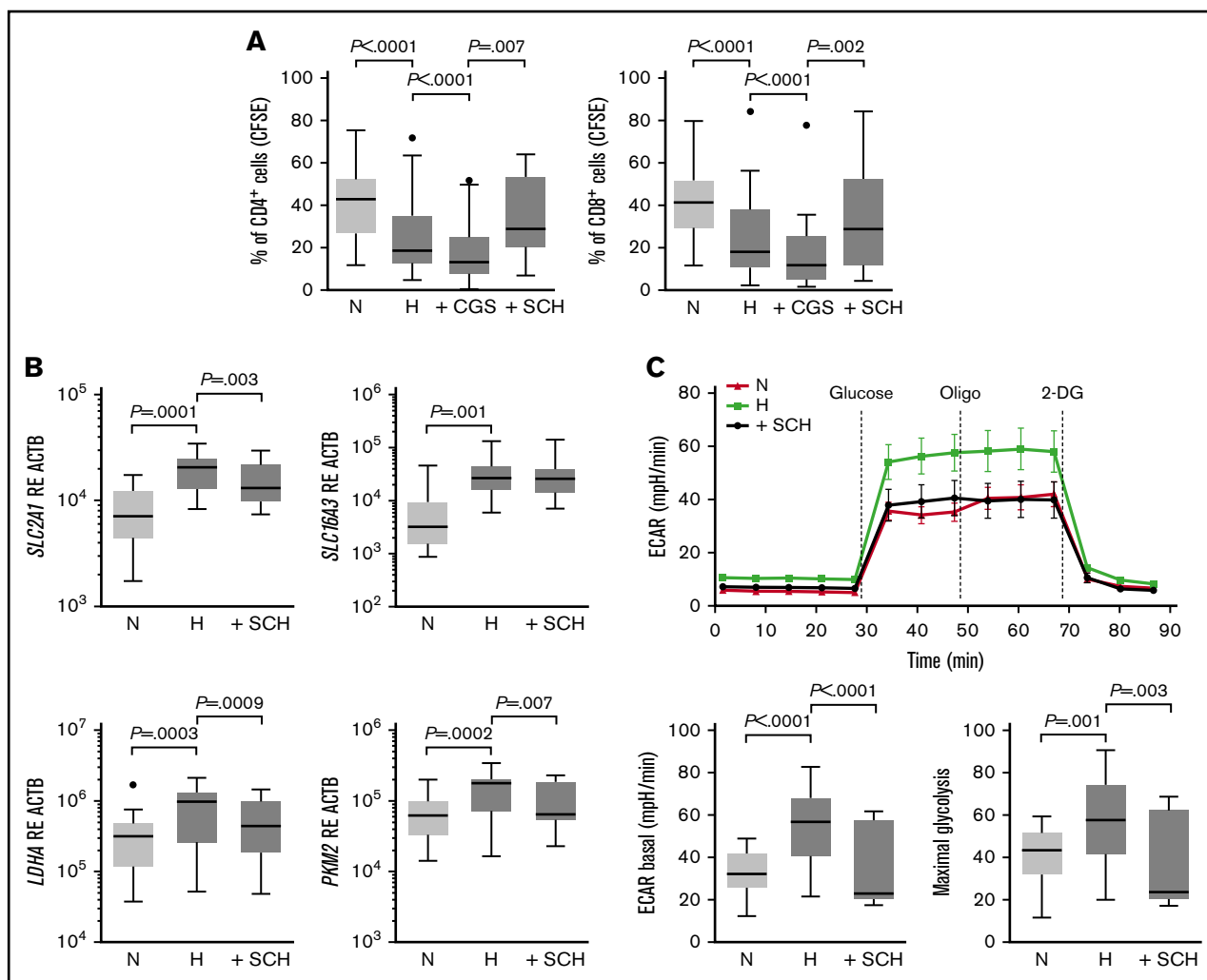


Figure 6. Hypoxia suppresses T-cell responses, and blockade of adenosine signaling can reverse the metabolic switch induced by hypoxia. (A) Cumulative data and representative carboxyfluorescein diacetate succinimidyl ester profiles of CD4⁺ (left panel, n = 19) and CD8⁺ (right panel, n = 19) cells after 3 days of culture in normoxia or hypoxia in the presence of anti-CD3 (0.5 μg/mL) and anti-CD28 (1 μg/mL) antibodies and the A2A agonist CGS21680 or antagonist SCH58261 (both at 1 μM, added at the beginning of culture). (B) RT-PCR studies showing expression of GLUT1 (*SLC2A1*) and MCT4 (*SLC16A3*, top panels), LDH (*LDHA*), and PKM2 (*PKM2*, bottom panels) in T lymphocytes sorted from PBMCs of 15 patients cultured for 5 days under normoxic or hypoxic conditions in the presence of anti-CD3 (2 μg/mL) and anti-CD28 (1 μg/mL) antibodies and IL-2 (100 U/mL). Where indicated, the A2A antagonist SCH58261 (10 μM) was added for the entire length of the experiment. (C) Bioenergetics profile (top panel) of dynamic measurement of the ECAR on activated T lymphocytes cultured for 5 days under normoxia or hypoxia with and without SCH58261 (10 μM). Glucose (10 mM), oligomycin (1 μM), and 2-DG (50 mM) were added as indicated by the dashed lines. Boxplots in the bottom panels show cumulative data of basal ECAR and maximal glycolysis (after glucose and oligo injection respectively) of CLL T lymphocytes (n = 4) obtained after activation and sorting as described above. Each experiment was performed in triplicate. Statistical differences were determined using the Wilcoxon signed rank and Mann-Whitney *U* tests followed by the Tukey test for panels A and B. B, basal; CGS, CGS21680; H, hypoxia (dark gray boxes); N, normoxia (light gray boxes); Oligo, oligomycin; SCH, SCH58261; 2-DG, 2-deoxy-D-glucose.

intensely IL-10⁺ T cells in the CLL LN indicates that this hypoxic circuit is activated in tissues (Figure 3G). Addition of the A2A antagonist impaired Treg generation, TGF-β induction, PD-1 expression, and IL-10 synthesis and secretion (Figure 7A-G).

Discussion

This study shows that the LN of CLL patients, in particular their proliferation centers, are characterized by overexpression and activation of HIF-1α. It also shows that activation of this transcriptional program favors tumor growth and survival while weakening immune responses by acting both on tumor and on bystander

cells. These effects are partially attributable to increased adenosine production and signaling via the A2A receptor, arguing in favor of its therapeutic targeting.

Several indications point to hypoxia as the main activator of HIF-1α expression and signaling. First, we observed a modest but highly significant gradient in the expression of CAIX, the HIF-1α target employed to stain LNs. CAIX positivity was less intense in the perivascular areas than in other parts of the tissue, suggesting that its expression is inversely correlated to the distance from the vessel. Secondly, we found that PIM, a compound that binds covalently to sulphhydryl group-containing molecules in hypoxic tissues, stained

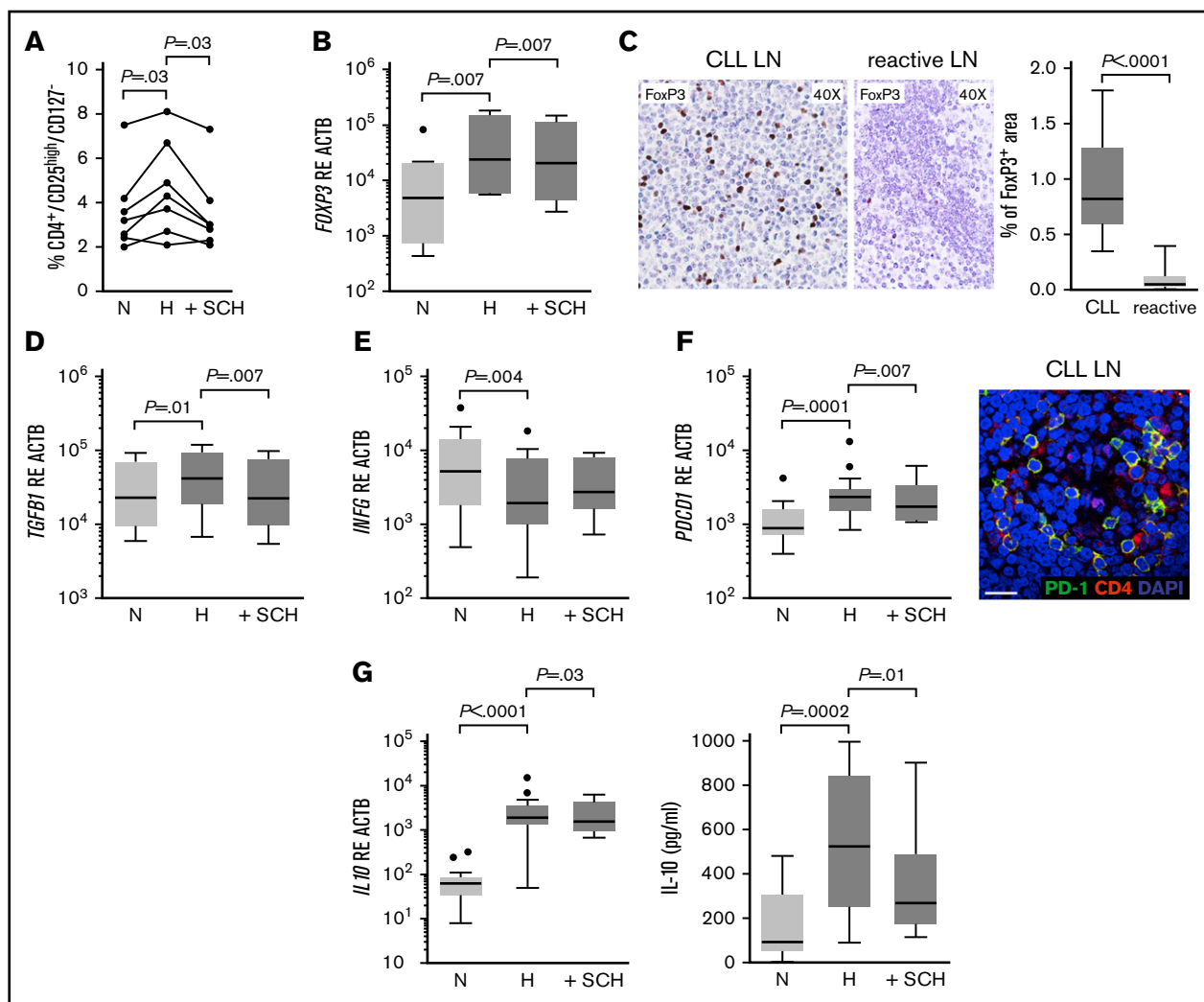


Figure 7. Hypoxia increases the number of Tregs with suppressive characteristics in an A2A-dependent manner. (A) Cumulative data of the percentage of $CD4^{+}/CD25^{high}/CD127^{-}$ cells evaluated in 7 randomly selected CLL patients after 3 days of culture under normoxia or hypoxia. Where indicated, the A2A antagonist SCH58261 ($10 \mu\text{M}$) was added for the entire experiment. (B) RT-PCR data showing an increased expression of FoxP3 (*FOXP3*, $n = 8$) in T lymphocytes purified from CLL PBMCs cultured for 5 days in the presence of anti-CD3 ($2 \mu\text{g}/\text{mL}$) and anti-CD28 ($1 \mu\text{g}/\text{mL}$) antibodies and IL-2 ($100 \text{ U}/\text{mL}$). Cultures were maintained at 21% or 1% O_2 . The A2A antagonist SCH58261 ($10 \mu\text{M}$) was added where indicated. (C) Representative immunohistochemical FoxP3 staining of CLL (left panel) and reactive (middle panel) LN sections indicating a greater number of FoxP3⁺ cells in the CLL LN compartment than in the reactive counterpart. Cumulative data on the percentage of FoxP3⁺ area confirmed statistical significant differences ($n = 20$, right panel). Original magnification $\times 40$. (D-F) RT-PCR data on the expression of TGF- $\beta 1$ (*TGF $\beta 1$* , $n = 10$; D), interferon γ (*IFNG*, $n = 10$; E), and the immunoinhibitory molecule PD-1 (*PDCD1*, $n = 10$; F, left panel) in sorted T cells after 5 days of normoxic and hypoxic culture under activated conditions. Antagonist SCH58261 ($10 \mu\text{M}$) was added where indicated. (F) Representative image showing PD-1 and CD4 co-localization in a typical CLL LN section. Original magnification $\times 63$. Scale bar, $25 \mu\text{m}$. (G) RT-PCR analysis of the IL-10 cytokine (*IL10*, $n = 10$) in T cells sorted from CLL patients after 5 days of normoxic and hypoxic culture with or without the A2A antagonist (left panel). Secretion of IL-10 was confirmed by ELISA of T-cell culture supernatants (right panel). SCH58261 ($10 \mu\text{M}$) was added for the entire experiment where indicated. Statistical differences were analyzed with the Wilcoxon signed rank and Mann-Whitney *U* tests followed by the Tukey test for panels B and E-G. H, hypoxia (dark gray boxes); N, normoxia (light gray boxes); SCH, SCH58261.

human leukemic infiltrates in spleen sections of a xenograft model of CLL.⁵⁴ Thirdly, in paired samples of PB, BM, and LN, we observed a gradient of expression of HIF-1 α and its targets, with highest levels in the LN, followed by BM and PB.^{55,56}

These findings led us to consider the possibility that hypoxia is functionally relevant for CLL cells. We therefore decided to investigate the consequences of hypoxia in leukemic cells and the main cellular components of the proliferation center. Under hypoxia, CLL cells rapidly adapted their metabolism by upregulating genes involved in glycolysis. This metabolic adaptation was recently

described for macrophages and T cells, where it was linked to increased survival and appearance of an immunosuppressive phenotype.^{40,43} Consistently, hypoxia protected CLL cells from drug-induced apoptosis and triggered production of IL-10, which is considered the hallmark cytokine for regulatory B cells.⁵⁷ Monocytes in hypoxic conditions differentiated more readily into M2 macrophages, becoming more efficient supporters of CLL survival, while T lymphocytes showed impaired proliferation and increased expression of Treg markers. The effects converged to create ideal conditions for tumor growth in closed environments. On one hand,

hypoxia made leukemic cells more resistant to environmental stresses and more responsive to proliferative signals. On the other hand, it modified bystander myeloid and T cells, depressing immune responses and enhancing tumor-supporting properties.

A common effect of hypoxia in the CLL niche was strong induction of adenosine production, which was generated mainly by macrophages. Macrophages differentiated under low O₂ tensions became strongly CD73⁺ and significantly upregulated their adenosine-producing capacity, without meaningful inosine conversion. Consequently, it appears that macrophages are the cells that produce the highest levels of extracellular adenosine in the CLL niche. The second major observation of this paper is that hypoxia strongly upregulates the A2A receptor in all cell types analyzed, including CLL cells, macrophages, and T lymphocytes. This finding suggests that macrophage-generated adenosine may have both autocrine and paracrine effects. Inhibitors of the A2A receptor reversed many of the hypoxia-induced effects, in a lineage-specific way. In CLL cells, we found that it prevented the glycolytic switch, restoring full responses to drugs and blocking IL-10 production. This mechanism may be linked to blockade of A2A signaling, with decreased intracellular cAMP levels in turn inhibiting cAMP-dependent protein kinase A (PKA). In line with this hypothesis, recent evidence⁵⁸ indicates that PKA is a HIF-1 α -interacting protein positively regulating expression of HIF-1 α target genes. Likewise, PKA-mediated activation of the transcription factor cAMP response element (CRE) binding protein (CREB) induces IL-10 production,⁵⁹ providing a direct link between A2A signaling and regulation of gene expression.

In macrophages, there are 2 observations that indicate that activation of the A2A receptor recapitulates the effects of hypoxia. First of all, the A2A agonist under normoxia promoted differentiation of macrophages with an alternatively activated phenotype and functional properties. Secondly, the antagonist used in hypoxic cultures partially reverted the hypoxia-induced phenotype. This is a relevant point, because it suggests that pharmacological modulation of the adenosine axis could revert the hypoxic phenotype. In T lymphocytes, inhibition of adenosine signaling using A2A inhibitors restored T-cell proliferation as well as secretion of Th1 cytokines. The finding in CLL LNs of exhausted T cells suggests that this is a relevant phenomenon in vivo and that therapeutic targeting of the adenosine axis could restore T-cell competence, as shown in other models.^{41,43,60,61}

Several labs have linked the adenosine axis to tumor transformation and have provided evidence that inhibition of adenosine production or signaling are effective in preventing tumor growth and/or diffusion.⁶²⁻⁶⁵ Monoclonal antibodies to CD39⁶⁶ and to

CD73⁶⁷ have shown preclinical efficacy in solid tumor models, as have antagonists of the adenosine receptors.⁶⁸ Another proposal is to increase O₂ concentrations throughout the body, thus preventing adenosine generation and subsequent signaling.⁶⁹ No matter what therapeutic strategy is adopted, inhibiting adenosine formation and signaling appears to be a sound approach to combating local conditions favorable to the tumor. A combination of "adenosine inhibition" therapies with drugs that directly target the tumor or restore immune functions, such as checkpoint inhibitors, could represent a winning strategy for a still-incurable disease such as CLL.

Acknowledgments

The authors thank Katuscia Gizzi for excellent technical support.

This work was supported by grants from the Associazione Italiana per la Ricerca sul Cancro (AIRC) (IG 12754 and 5x1000 100007), the Italian Ministries of Education, University and Research (Futuro in Ricerca 2012 RBFR12D1CB), the Italian Ministry of Health (Bando Giovani Ricercatori GR-2011-02346826 and GR-2011-02349282 and Bando Ricerca Finalizzata RF-2011-02349712), the Fondazione Cariplo (2012-0689), and local university funds (60%). V.A. is supported by a triennial Fondazione Italiana per la Ricerca sul Cancro/AIRC fellowship (15047).

Authorship

Contribution: S.S. designed the study, performed experiments, and analyzed and interpreted data; T.V., V.A., C.B., R.B., F.A., and D.B. performed experiments and analyzed data; O.J. provided paired (PB-BM-LN) patient samples; G.I. provided LN sections; M.C., D.R., R.R.F., and G.G. provided patient samples and relevant clinical information; S.C.R. contributed to data interpretation; S.-S.C. and N.C. performed xenograft experiments, provided mouse spleen sections and purified human cells, and contributed to data interpretation; and S.D. designed the study, interpreted data, and wrote the paper.

Conflict-of-interest disclosure: The authors declare that there is no conflict of interest.

The current affiliation for D.R. is Hematology, Oncology Institute of Southern Switzerland, and Institute of Oncology Research, Bellinzona, Switzerland.

ORCID profiles: S.S., 0000-0003-0399-6539; S.D., 0000-0003-0632-5036.

Correspondence: Silvia Deaglio, Department of Medical Sciences, University of Turin School of Medicine & Human Genetics Foundation, via Nizza, 52, 10126 Turin, Italy; e-mail: silvia.deaglio@unito.it or silvia.deaglio@hugef-torino.org.

References

1. Chiorazzi N, Rai KR, Ferrarini M. Chronic lymphocytic leukemia. *N Engl J Med*. 2005;352(8):804-815.
2. Messmer BT, Messmer D, Allen SL, et al. In vivo measurements document the dynamic cellular kinetics of chronic lymphocytic leukemia B cells. *J Clin Invest*. 2005;115(3):755-764.
3. Burger JA, Ghia P, Rosenwald A, Caligaris-Cappio F. The microenvironment in mature B-cell malignancies: a target for new treatment strategies. *Blood*. 2009;114(16):3367-3375.
4. Ponzoni M, Doglioni C, Caligaris-Cappio F. Chronic lymphocytic leukemia: the pathologist's view of lymph node microenvironment. *Semin Diagn Pathol*. 2011;28(2):161-166.

5. Ten Hacken E, Burger JA. Microenvironment interactions and B-cell receptor signaling in chronic lymphocytic leukemia: implications for disease pathogenesis and treatment. *Biochim Biophys Acta*. 2016;1863(3):401-413.
6. Byrd JC, Brown JR, O'Brien S, et al. Ibrutinib versus ofatumumab in previously treated chronic lymphoid leukemia. *N Engl J Med*. 2014;371(3):213-223.
7. Furman RR, Sharman JP, Coutre SE, et al. Idelalisib and rituximab in relapsed chronic lymphocytic leukemia. *N Engl J Med*. 2014;370(11):997-1007.
8. Burnstock G. Purinergic signalling: Its unpopular beginning, its acceptance and its exciting future. *BioEssays*. 2012;34(3):218-225.
9. Pellegatti P, Raffaghello L, Bianchi G, Piccardi F, Pistoia V, Di Virgilio F. Increased level of extracellular ATP at tumor sites: in vivo imaging with plasma membrane luciferase. *PLoS One*. 2008;3(7):e2599.
10. Stagg J, Smyth MJ. Extracellular adenosine triphosphate and adenosine in cancer. *Oncogene*. 2010;29(39):5346-5358.
11. Resta R, Yamashita Y, Thompson LF. Ecto-enzyme and signaling functions of lymphocyte CD73. *Immunol Rev*. 1998;161:95-109.
12. Mikhailov A, Sokolovskaya A, Yegutkin GG, et al. CD73 participates in cellular multiresistance program and protects against TRAIL-induced apoptosis. *J Immunol*. 2008;181(1):464-475.
13. Young A, Mittal D, Stannard K, et al. Co-blockade of immune checkpoints and adenosine A_{2A} receptor suppresses metastasis. *Oncol Immunology*. 2014;3(10):e958952.
14. Serra S, Horenstein AL, Vaisitti T, et al. CD73-generated extracellular adenosine in chronic lymphocytic leukemia creates local conditions counteracting drug-induced cell death. *Blood*. 2011;118(23):6141-6152.
15. Synnestvedt K, Furuta GT, Comerford KM, et al. Ecto-5'-nucleotidase (CD73) regulation by hypoxia-inducible factor-1 mediates permeability changes in intestinal epithelia. *J Clin Invest*. 2002;110(7):993-1002.
16. Keith B, Johnson RS, Simon MC. HIF1alpha and HIF2alpha: sibling rivalry in hypoxic tumour growth and progression. *Nat Rev Cancer*. 2012;12(1):9-22.
17. Shachar I, Cohen S, Marom A, Becker-Herman S. Regulation of CLL survival by hypoxia-inducible factor and its target genes. *FEBS Lett*. 2012;586(18):2906-2910.
18. Sitkovsky MV. T regulatory cells: hypoxia-adenosinergic suppression and re-direction of the immune response. *Trends Immunol*. 2009;30(3):102-108.
19. Benito J, Shi Y, Szymanska B, et al. Pronounced hypoxia in models of murine and human leukemia: high efficacy of hypoxia-activated prodrug PR-104. *PLoS One*. 2011;6(8):e23108.
20. Ghosh AK, Shanafelt TD, Cimmino A, et al. Aberrant regulation of pVHL levels by microRNA promotes the HIF/VEGF axis in CLL B cells. *Blood*. 2009;113(22):5568-5574.
21. Valsecchi R, Coltella N, Belloni D, et al. HIF-1alpha regulates the interaction of chronic lymphocytic leukemia cells with the tumor microenvironment. *Blood*. 2016;127(16):1987-1997.
22. Sitkovsky MV, Kjaergaard J, Lukashev D, Ohta A. Hypoxia-adenosinergic immunosuppression: tumor protection by T regulatory cells and cancerous tissue hypoxia. *Clin Cancer Res*. 2008;14(19):5947-5952.
23. Semenza GL. Defining the role of hypoxia-inducible factor 1 in cancer biology and therapeutics. *Oncogene*. 2010;29(5):625-634.
24. Deaglio S, Vaisitti T, Aydin S, et al. CD38 and ZAP-70 are functionally linked and mark CLL cells with high migratory potential. *Blood*. 2007;110(12):4012-4021.
25. Airley RE, Loncaster J, Raleigh JA, et al. GLUT-1 and CAIX as intrinsic markers of hypoxia in carcinoma of the cervix: relationship to pimonidazole binding. *Int J Cancer*. 2003;104(1):85-91.
26. Gross MW, Karbach U, Groebe K, Franko AJ, Mueller-Klieser W. Calibration of misonidazole labeling by simultaneous measurement of oxygen tension and labeling density in multicellular spheroids. *Int J Cancer*. 1995;61(4):567-573.
27. Marín-Hernández A, Gallardo-Perez JC, Ralph SJ, Rodriguez-Enriquez S, Moreno-Sanchez R. HIF-1alpha modulates energy metabolism in cancer cells by inducing over-expression of specific glycolytic isoforms. *Mini Rev Med Chem*. 2009;9(9):1084-1101.
28. Semenza GL. HIF-1: upstream and downstream of cancer metabolism. *Curr Opin Genet Dev*. 2010;20(1):51-56.
29. Iqbal MA, Gupta V, Gopinath P, Mazurek S, Bamezai RN. Pyruvate kinase M2 and cancer: an updated assessment. *FEBS Lett*. 2014;588(16):2685-2692.
30. Sitkovsky MV, Lukashev D, Apasov S, et al. Physiological control of immune response and inflammatory tissue damage by hypoxia-inducible factors and adenosine A_{2A} receptors. *Annu Rev Immunol*. 2004;22:657-682.
31. Poth JM, Brodsky K, Ehrentraut H, Grenz A, Eitzschig HK. Transcriptional control of adenosine signaling by hypoxia-inducible transcription factors during ischemic or inflammatory disease. *J Mol Med (Berl)*. 2013;91(2):183-193.
32. Damle RN, Ghiotto F, Valetto A, et al. B-cell chronic lymphocytic leukemia cells express a surface membrane phenotype of activated, antigen-experienced B lymphocytes. *Blood*. 2002;99(11):4087-4093.
33. Cortés A, Gracia E, Moreno E, et al. Moonlighting adenosine deaminase: a target protein for drug development. *Med Res Rev*. 2015;35(1):85-125.
34. Semenza GL. HIF-1 mediates metabolic responses to intratumoral hypoxia and oncogenic mutations. *J Clin Invest*. 2013;123(9):3664-3671.
35. Ohta A. A metabolic immune checkpoint: adenosine in tumor microenvironment. *Front Immunol*. 2016;7:109.
36. Eckle T, Hartmann K, Bonney S, et al. Adora2b-elicited Per2 stabilization promotes a HIF-dependent metabolic switch crucial for myocardial adaptation to ischemia. *Nat Med*. 2012;18(5):774-782.
37. Eckle T, Kewley EM, Brodsky KS, et al. Identification of hypoxia-inducible factor HIF-1A as transcriptional regulator of the A_{2B} adenosine receptor during acute lung injury. *J Immunol*. 2014;192(3):1249-1256.

38. Jitschin R, Hofmann AD, Bruns H, et al. Mitochondrial metabolism contributes to oxidative stress and reveals therapeutic targets in chronic lymphocytic leukemia. *Blood*. 2014;123(17):2663-2672.
39. Koczula KM, Ludwig C, Hayden R, et al. Metabolic plasticity in CLL: adaptation to the hypoxic niche. *Leukemia*. 2016;30(1):65-73.
40. Krawczyk CM, Holowka T, Sun J, et al. Toll-like receptor-induced changes in glycolytic metabolism regulate dendritic cell activation. *Blood*. 2010;115(23):4742-4749.
41. De Rosa V, Galgani M, Porcellini A, et al. Glycolysis controls the induction of human regulatory T cells by modulating the expression of FOXP3 exon 2 splicing variants. *Nat Immunol*. 2015;16(11):1174-1184.
42. Panther E, Corinti S, Idzko M, et al. Adenosine affects expression of membrane molecules, cytokine and chemokine release, and the T-cell stimulatory capacity of human dendritic cells. *Blood*. 2003;101(10):3985-3990.
43. Mascanfroni ID, Takenaka MC, Yeste A, et al. Metabolic control of type 1 regulatory T cell differentiation by AHR and HIF1- α . *Nat Med*. 2015;21(6):638-646.
44. DiLillo DJ, Weinberg JB, Yoshizaki A, et al. Chronic lymphocytic leukemia and regulatory B cells share IL-10 competence and immunosuppressive function. *Leukemia*. 2013;27(1):170-182.
45. Burger JA, Gribben JG. The microenvironment in chronic lymphocytic leukemia (CLL) and other B cell malignancies: insight into disease biology and new targeted therapies. *Semin Cancer Biol*. 2014;24:71-81.
46. Boissard F, Fournie JJ, Laurent C, Poupot M, Ysebaert L. Nurse like cells: chronic lymphocytic leukemia associated macrophages. *Leuk Lymphoma*. 2015;56(5):1570-1572.
47. Audrito V, Serra S, Brusa D, et al. Extracellular nicotinamide phosphoribosyltransferase (NAMPT) promotes M2 macrophage polarization in chronic lymphocytic leukemia. *Blood*. 2015;125(1):111-123.
48. Sica A, Mantovani A. Macrophage plasticity and polarization: in vivo veritas. *J Clin Invest*. 2012;122(3):787-795.
49. Ohta A, Sitkovsky M. Extracellular adenosine-mediated modulation of regulatory T cells. *Front Immunol*. 2014;5:304.
50. Pearce EL, Poffenberger MC, Chang CH, Jones RG. Fueling immunity: insights into metabolism and lymphocyte function. *Science*. 2013;342(6155):1242-1245.
51. Chang JT, Wherry EJ, Goldrath AW. Molecular regulation of effector and memory T cell differentiation. *Nat Immunol*. 2014;15(12):1104-1115.
52. Chen W, Jin W, Hardegen N, et al. Conversion of peripheral CD4⁺CD25⁻ naive T cells to CD4⁺CD25⁺ regulatory T cells by TGF- β induction of transcription factor Foxp3. *J Exp Med*. 2003;198(12):1875-1886.
53. Brusa D, Serra S, Coscia M, et al. The PD-1/PD-L1 axis contributes to T-cell dysfunction in chronic lymphocytic leukemia. *Haematologica*. 2013;98(6):953-963.
54. Bagnara D, Kaufman MS, Calissano C, et al. A novel adoptive transfer model of chronic lymphocytic leukemia suggests a key role for T lymphocytes in the disease. *Blood*. 2011;117(20):5463-5472.
55. Chen SS, Chiorazzi N. Murine genetically engineered and human xenograft models of chronic lymphocytic leukemia. *Semin Hematol*. 2014;51(3):188-205.
56. Patten PE, Ferrer G, Chen SS, et al. Chronic lymphocytic leukemia cells diversify and differentiate in vivo via a nonclassical Th1-dependent, Bcl-6-deficient process. *JCI Insight*. 2016;1(4).
57. Saulep-Easton D, Vincent FB, Quah PS, et al. The BAFF receptor TACI controls IL-10 production by regulatory B cells and CLL B cells. *Leukemia*. 2016;30(1):163-172.
58. Bullen JW, Tchernyshyov I, Holewinski RJ, et al. Protein kinase A-dependent phosphorylation stimulates the transcriptional activity of hypoxia-inducible factor 1. *Sci Signal*. 2016;9(430):ra56.
59. Wen AY, Sakamoto KM, Miller LS. The role of the transcription factor CREB in immune function. *J Immunol*. 2010;185(11):6413-6419.
60. Kojima H, Gu H, Nomura S, et al. Abnormal B lymphocyte development and autoimmunity in hypoxia-inducible factor 1 α -deficient chimeric mice. *Proc Natl Acad Sci USA*. 2002;99(4):2170-2174.
61. Lukashev D, Klebanov B, Kojima H, et al. Cutting edge: hypoxia-inducible factor 1 α and its activation-inducible short isoform I.1 negatively regulate functions of CD4⁺ and CD8⁺ T lymphocytes. *J Immunol*. 2006;177(8):4962-4965.
62. Ohta A, Sitkovsky M. Role of G-protein-coupled adenosine receptors in downregulation of inflammation and protection from tissue damage. *Nature*. 2001;414(6866):916-920.
63. Thiel M, Chouker A, Ohta A, et al. Oxygenation inhibits the physiological tissue-protecting mechanism and thereby exacerbates acute inflammatory lung injury. *PLoS Biol*. 2005;3(6):e174.
64. Ohta A, Gorelik E, Prasad SJ, et al. A2A adenosine receptor protects tumors from antitumor T cells. *Proc Natl Acad Sci USA*. 2006;103(35):13132-13137.
65. Young A, Mittal D, Stagg J, Smyth MJ. Targeting cancer-derived adenosine: new therapeutic approaches. *Cancer Discov*. 2014;4(8):879-888.
66. Bastid J, Cottalorda-Regairaz A, Alberici G, Bonnefoy N, Eliaou JF, Bensussan A. ENTPD1/CD39 is a promising therapeutic target in oncology. *Oncogene*. 2013;32(14):1743-1751.
67. Stagg J, Divisekera U, McLaughlin N, et al. Anti-CD73 antibody therapy inhibits breast tumor growth and metastasis. *Proc Natl Acad Sci USA*. 2010;107(4):1547-1552.
68. Beavis PA, Divisekera U, Paget C, et al. Blockade of A2A receptors potently suppresses the metastasis of CD73⁺ tumors. *Proc Natl Acad Sci USA*. 2013;110(36):14711-14716.
69. Hatfield SM, Kjaergaard J, Lukashev D, et al. Immunological mechanisms of the antitumor effects of supplemental oxygenation. *Sci Transl Med*. 2015;7(277):277ra230.